



CrossMark
click for updates

Cite this: *RSC Adv.*, 2015, 5, 8938

Received 25th October 2014
Accepted 16th December 2014

DOI: 10.1039/c4ra13135e

www.rsc.org/advances

A dual targeting cyclodextrin/gold nanoparticle conjugate as a scaffold for solubilization and delivery of paclitaxel†

Yong Chen, Nan Li, Yang Yang and Yu Liu*

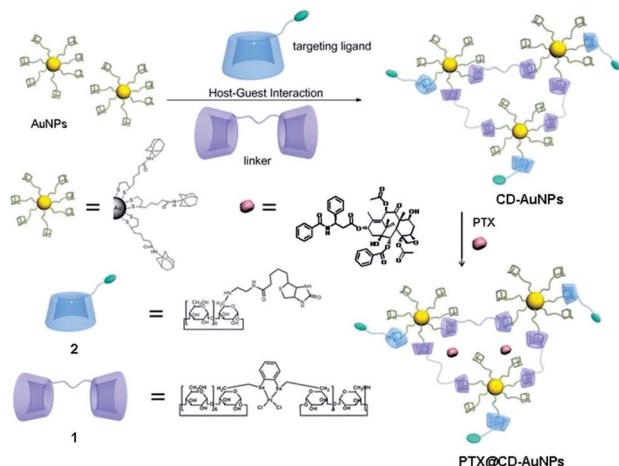
Recently, the improvement of the aqueous solubility, biocompatibility, and targeted delivery effects of drug carriers became research highlights in the field of cancer therapy. A novel cyclodextrin–gold nanoparticle conjugate, CD–AuNPs, was successfully constructed from gold nanoparticles (AuNPs) bearing adamantane moieties, shortly linked cyclodextrin dimmers, and biotin-modified cyclodextrin. Possessing a holey structure, the resultant conjugate could serve as a versatile and biocompatible platform for the loading and solubilization of paclitaxel. In addition, the active targeting of biotin units and the pH-responsive accelerated drug release in a mildly acidic environment like that in cancer cells efficiently promote the advantage of CD–AuNPs as a dual targeting delivery carrier for paclitaxel, giving better anti-cancer activity and lower toxicity toward normal cells than free paclitaxel. We believe that the present work will provide a new pathway to the design of a novel targeted drug carrier.

Among the various building blocks used to construct bioactive organic–inorganic hybrid materials,¹ cyclodextrins or gold nanoparticles are widely regarded as one of the best candidates from the organic or inorganic side, respectively. Cyclodextrins (CDs), a series of cyclic oligosaccharides, are water-soluble, non-toxic, commercially available with low price, and their well-defined hydrophobic cavity can bind various organic/biological substrates to construct nanostructured functional supramolecular assemblies especially as bioactive materials.² On the other hand, compared to traditional drug delivery materials, such as liposomes³ and polymeric micelles,⁴ gold nanoparticles are widely regarded as one of the best candidates of drug carriers,^{5,6} owing to a number of desirable advantages including (1) biocompatibility and low cytotoxicity;⁷ (2) convenient synthesis and easy size control;⁸ (3) robust stability under most *in vivo* conditions;⁹ and (4) tunable surface features and

dense loading functionalities for specific cell targeting.¹⁰ Thus, one can believe that the combination of cyclodextrins with gold nanoparticles, accompanied by the introduction of an additional targeting site, will be developed into a new approach to delivery bioactive molecules.¹¹ Kim *et al.* reported a β -CD-covered gold nanoparticles bearing anti-epidermal growth factor receptor antibody as a carrier of anticancer drug β -lapachone.¹² Kwon *et al.* reported that gold nanoparticles surface-functionalized PEG, biotin and rhodamine B linked β -CD can be effectively involved with the cancer cells.¹³ Vargas-Berenguel *et al.* reported several β -CD-bearing gold glyconanoparticles with human galectin-3 (Gal-3) targeting moiety as a carrier of anticancer drug methotrexate.¹⁴ The drug loading of these systems mainly involves the encapsulation of the β -CD cavity towards anti-cancer drugs. Therefore, the relatively low to moderate binding ability of the monoric β -CD cavity with drug molecules will inevitably disfavor their applications. Recently, we reported a polysaccharide–gold nanocluster supramolecular conjugate (HACD–AuNPs) that possesses a holey structure as a versatile platform for the loading and delivery of various anti-cancer drugs from gold nanoparticles and cyclodextrin-grafted hyaluronic acid.¹⁵ In the present work, we construct a new cyclodextrin/gold nanoparticle conjugate (CD–AuNPs) from gold nanoparticles (AuNPs) bearing adamantane moieties and 6,6'-(*o*-phenylenediseleno)-bridged bis(β -CD) (Scheme 1), where the shortly linked bis(β -CD)s are used instead of hyaluronic acid macromolecules to increase the loading efficiency of the conjugate. Moreover, biotin (vitamin B7), a growth promoter at the cellular level whose receptors are overexpressed on the surface of cancer cells,¹⁶ was also introduced to the conjugate as an active targeting site. In addition, the different binding abilities of the β -CD cavity with adamantane at different pH values also led to the accelerated release of drug in cancer cells.^{2a} It is noteworthy that paclitaxel (PTX) is widely regarded as one of the most effective drugs for treating various cancers.¹⁷ However, the therapeutic effects of PTX are greatly limited because of its poor water-solubility and the lack of targeting towards cancer cells, leading to toxic side effects on normal cells.¹⁸ Significantly, PTX

Department of Chemistry, State Key Laboratory of Elemento-Organic Chemistry, Collaborative Innovation Center of Chemical Science and Engineering (Tianjin), Nankai University, Tianjin 300071, P.R. China. E-mail: yuliu@nankai.edu.cn

† Electronic supplementary information (ESI) available. See DOI: 10.1039/c4ra13135e



Scheme 1 Chemical structures and construction of CD-AuNPs and drug@CD-AuNPs.

could be efficiently loaded in the three-dimensional holey structure of CD-AuNPs, resulting in the enhanced water solubility, improved anti-cancer activity and decreased toxic side effects of the drug@CD-AuNP conjugate as compared with free PTX. In addition, compared with other drug delivery systems, especially our previously reported HACD-AuNP system, the present CD-AuNP system showed a certain advantage for the targeting effect, biocompatibility, drug solubilization ability, and drug loading efficiency of a supramolecular conjugate, which was definitely beneficial in the targeted drug delivery and the controlled release of PTX.

Benefitting from the strong binding between the β -CD cavity and adamantane moiety attached to the surface of gold nanoparticles,¹⁴ CD-AuNPs, which showed satisfactory water solubility, could be easily constructed *in situ* by mixing 1, 2 and AuNPs in solution. From the ¹H NMR spectrum of CD-AuNPs in D₂O, a comparison of the integral area of proton peaks indicated that the molar ratio between 1 and 2 was *ca.* 5 : 1, and the molecular ratio between the adamantane moiety and β -CD cavity was 1 : 1. Therefore, the number of β -CDs on each AuNP was estimated to be 19, because the average number of adamantane moieties on the surface of each AuNP was calculated to be 19 according to a previous report.¹⁵ As compared with the UV-vis spectrum of AuNPs in water, which showed a characteristic absorption peak at 514 nm for the surface plasmon resonance (SPR) absorption,¹⁹ the SPR maximum of CD-AuNPs was obviously shifted to *ca.* 548 nm, probably indicating that gold nanoparticles had aggregated into larger clusters or the thickness of the adsorbed molecules increased.²⁰ In addition, TEM images of AuNPs (Fig. 1a) showed a number of well dispersed spherical particles with an average diameter of 2.2 nm. After the addition of 2, the size and shape of AuNPs remained unchanged (Fig. 1b). However, with the addition of 1 and 2, the originally discrete gold particles in the TEM image of AuNPs aggregated to form large clusters in the TEM image of CD-AuNPs (Fig. 1c), and these large nanoclusters dissembled into discrete nanoparticles, which is quite similar to the image of free AuNPs in

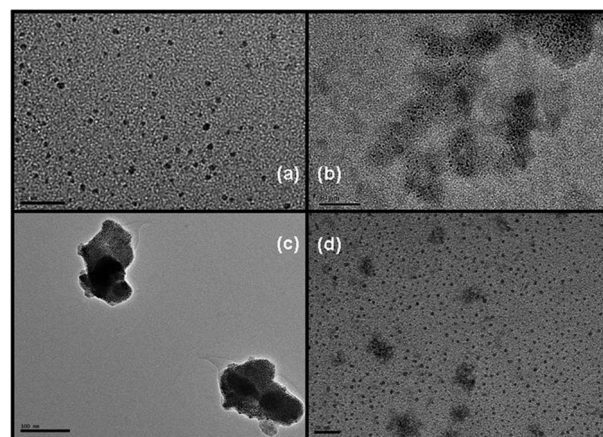


Fig. 1 (a) HR-TEM image of AuNPs (scale bar = 20 nm), (b) 2 + AuNPs (scale bar = 50 nm), (c) CD-AuNPs (scale bar = 100 nm), and (d) CD-AuNPs in the presence of ethanol (scale bar = 20 nm).

the presence of ethanol (Fig. 1d). A possible reason may be that CDs are reported to barely include the guest molecule in ethanol, and the exclusion of the included adamantane moiety of AuNPs from CD cavities of 1 or 2 will inevitably take place in an ethanol solution. These results demonstrated that the construction of CD-AuNPs was mainly driven by non-covalent weak interactions.

Similar structural information for CD-AuNPs comes from dynamic light scattering (DLS) experiments. The DLS data illustrated the large nanoclusters of CD-AuNPs with an average diameter of *ca.* 189 nm and a narrow size distribution (see ESI†).

As a water-soluble drug carrier, an important and desirable property of CD-AuNPs is its loading and controlled releasing ability towards drug molecules. In a typical example, the anti-cancer drug paclitaxel (PTX) was selected as a model drug. By measuring the characteristic absorption of PTX at 227 nm, the photometric standard curve of PTX was obtained with the absorption intensity as the ordinate and the PTX concentration in Milli-Q water solution as the abscissa. Accordingly, the PTX encapsulation efficiency of CD-AuNPs was calculated to be 77.5%, which is similar to that of previously reported HACD-AuNPs, but the loading efficiency of CD-AuNPs reached 19.4%, which is nearly twice as high as the corresponding value for HACD-AuNPs. In addition, the zeta potential of PTX@CD-AuNPs was measured to be *ca.* -8.24 mV, which is lower than that of CD-AuNPs (-13.54 mV), because the loaded PTX partly shielded the surface charge of CD-AuNPs. It is also noteworthy that, even after the loading of PTX, CD-AuNPs still maintained the negative charge on the surface, which would diminish the toxicity of the gold nanoparticles.^{9,21} Moreover, the PTX@CD-AuNPs were found to be stable in water and PBS for several months without obvious precipitation. These results jointly indicate that the anticancer drug PTX was efficiently loaded onto CD-AuNPs to form a biocompatible PTX@CD-AuNPs conjugate, which clearly demonstrates the possibility of applying CD-AuNPs as a convenient platform for the delivery of anticancer drugs.

It was also important to investigate the release behavior of PTX@CD–AuNPs, because a very important characteristic feature of a drug carrier is its controlled release in a physiological environment. The drug release profiles of PTX@CD–AuNPs in phosphate buffer solutions ($I = 0.01 \text{ M}$) at 37°C are presented in Fig. S9,[†] wherein different pH values (pH = 5.7 and 7.2) were selected for drug release because they are close to the physiological pH and the endosomal pH of cancer cells, respectively. The results showed that PTX@CD–AuNPs presented a slow and controlled release of PTX at pH 7.2 (physiological pH), and the release rate of PTX at pH 5.7 (endosomal pH of cancer cell) was nearly twice as high as that at pH 7.2. In the control experiment, free PTX showed no appreciable release under the same condition due to its poor water solubility. In another test, the sequential release behavior of PTX at different pH values was evaluated through UV-vis spectroscopy. As shown in Fig. S10,[†] a relatively low release of entrapped PTX was observed at pH 7.2 over periods of 75 min, indicating that PTX@CD–AuNP are stable toward leakage at physiological pH. However, the release rate was significantly enhanced when the environmental pH was changed to 5.7, demonstrating the pH-triggered release of PTX. About 20% of PTX was released in the first 75 min at pH 7.2, but rapidly reached 50% within 10 min after the pH value changed to 5.7. This pH-responsive preferred release of a drug in the cancer cell environment may be due to the weakened binding of the β -CD cavity with adamantane in an acidic environment, leading to the disassembly of CD–AuNPs, which will be helpful to not only improve the cytotoxic efficacy against tumor cells but also reduce toxicity of the drug to the normal tissue.²² In addition, this phenomenon also renders the present CD–AuNPs an intriguing targeted-delivery carrier of PTX, which encapsulates drug molecules to protect the active ingredient from premature degradation, and accelerates drug release when entering cancer cells.

Cytotoxicity experiments were performed to evaluate the cancer cell targeting and anticancer activity of PTX@CD–AuNPs *in vitro*, where a human ovarian cancer cell line SKOV-3 that abundantly over-expresses biotin receptors on the surface and mouse embryo NIH3T3 fibroblast cells that are biotin receptor-negative were selected as model cell lines. As shown in Fig. 2, PTX@CD–AuNPs displayed similar anticancer activity (relative cellular viability 61% vs. 65%) with that of free PTX after 24 h incubation, probably due to the specific association between biotin units on PTX@CD–AuNPs and biotin receptors on the cell surface, facilitating the incorporation of PTX@CD–AuNPs into the cancer cells by a biotin-mediated endocytosis process²³ and the subsequent preferred release of PTX at the endosomal pH of the cancer cell. This result is a little better than the previous result of DOX@HACD–AuNPs that also showed similar anticancer activity (relative cellular viability 53% vs. 46%) to free DOX.¹⁵ Only with the pH-responsive release of PTX but lacking the targeting effect of biotin, the anticancer activity of PTX@CD–AuNPs decreased by 21% when the biotin receptors of SKOV-3 cells were bound by an excess amount of biotin. For the normal NIH3T3 cells, the relative cellular viability upon

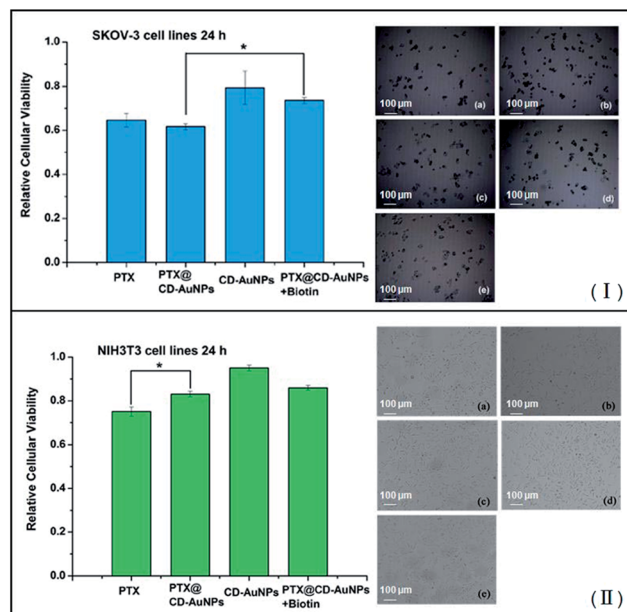


Fig. 2 Cytotoxicity experiments *in vitro* over 24 h. Relative cellular viability of SKOV-3 cell lines (I, left) and NIH3T3 cell lines (II, left) after 24 h. Images of SKOV-3 cell lines (I, right) and NIH3T3 cell lines (II, right) treated with (a) PTX, (b) PTX@CD–AuNPs, (c) CD–AuNPs, (d) PTX@CD–AuNPs + biotin and (e) blank are shown. The differences between PTX@CD–AuNPs and PTX@CD–AuNPs + Biotin in SKOV-3 cells over 24 h, PTX and PTX@CD–AuNPs in NIH3T3 cells over 24 h, which are indicated as statistically significant with asterisks ($P < 0.01$).

exposure to PTX@CD–AuNPs stayed at 83% after 24 h, which was higher than that of cells exposed to free PTX (75%). This indicates that the PTX@CD–AuNPs are less toxic to normal cells than free PTX. In the control experiment, CD–AuNPs showed nearly no cytotoxicity toward the NIH3T3 cells but slight cytotoxicity towards SKOV-3 cells. In addition, the morphological changes of cancer and normal cells revealed that PTX@CD–AuNPs more effectively damaged the cancer cells, but showed less toxicity towards normal cells than free PTX. This result is fully consistent with that obtained in the cell-counting experiments. Furthermore, the viability data at 48 h (see ESI[†]) showed similar positive results to those obtained at 24 h, verifying the conclusions mentioned earlier.

In summary, we developed a new drug delivery system with dual targeting by loading an anticancer drug PTX onto CD–AuNPs. Owing to the active targeting of biotin units and the pH-responsive drug release in cancer cells, the resultant PTX@CD–AuNPs exhibited better anti-cancer activity and the lower toxicity toward normal cells than free PTX. These results will promote CD–AuNPs as a useful carrier, providing novel possibilities for the development of targeted drug delivery and biomedical applications.

Acknowledgements

We thank 973 Program (2011CB932502) and NNSFC (91227107, 21432004, and 21272125) for financial support.

Notes and references

- 1 (a) J. Wu, N. Kamaly, J. Shi, L. Zhao, Z. Xiao, G. Hollett, R. John, S. Ray, X. Xu, X. Zhang, P. W. Kantoff and O. C. Farokhzad, *Angew. Chem., Int. Ed.*, 2014, **53**, 8975; (b) A. S. Campbell, C. Dong, F. Meng, J. Hardinger, G. Perhinschi, N. Wu and C. Z. Dinu, *ACS Appl. Mater. Interfaces*, 2014, **6**, 5393; (c) A. S. Campbell, C. Dong, J. S. Dordick and C. Z. Dinu, *Process Biochem.*, 2013, **48**, 1355.
- 2 (a) M. V. Rekharsky and Y. Inoue, *Chem. Rev.*, 1998, **98**, 1875; (b) K. Uekama, F. Hirayama and T. Irie, *Chem. Rev.*, 1998, **98**, 2045; (c) Y. Chen and Y. Liu, *Chem. Soc. Rev.*, 2010, **39**, 495.
- 3 (a) Y. Liu, J. Fang, Y.-J. Kim, M. K. Wong and P. Wang, *Mol. Pharm.*, 2014, **11**, 1651; (b) Z. Yu, R. M. Schmaltz, T. C. Bozeman, R. Paul, M. J. Rishel, K. S. Tsosie and S. M. Hecht, *J. Am. Chem. Soc.*, 2013, **135**, 2883.
- 4 H. H. Dam and F. Caruso, *Adv. Mater.*, 2011, **23**, 3026.
- 5 J. Song, J.-J. Zhou and H.-W. Duan, *J. Am. Chem. Soc.*, 2012, **134**, 13458.
- 6 H.-Y. Zhou, G.-X. Su, P.-F. Jiao and B. Yan, *Chem.-Eur. J.*, 2012, **18**, 5501.
- 7 S. K. Nune, N. Chanda, R. Shukla, K. Katti, R. R. Kulkarni, S. Thilakavathy, S. Mekapothula, R. Kannan and K. V. Katti, *J. Mater. Chem.*, 2009, **19**, 2912.
- 8 M. C. Daniel and D. Astruc, *Chem. Rev.*, 2004, **104**, 293.
- 9 D. A. Giljohann, D. S. Seferos, W. L. Daniel, M. D. Massich, P. C. Patel and C. A. Mirkin, *Angew. Chem., Int. Ed.*, 2010, **49**, 3280.
- 10 J. C. Love, J. A. Estroff, J. K. Kriebel, R. G. Nuzzo and G. M. Whitesides, *Chem. Rev.*, 2005, **105**, 1103.
- 11 (a) Y. W. Yang, Y.-L. Sun and N. Song, *Acc. Chem. Res.*, 2014, **47**, 1950; (b) L. Wang, L.-L. Li, Y.-S. Fan and H. Wang, *Adv. Mater.*, 2013, **25**, 3888; (c) Y. Chen, Y.-M. Zhang and Y. Liu, *Chem. Commun.*, 2010, **46**, 5622.
- 12 C. Park, H. Youn, H. Kim, T. Noh, Y. H. Kook, E. T. Oh, H. J. Park and C. Kim, *J. Mater. Chem.*, 2009, **19**, 2310.
- 13 D. N. Heo, D. H. Yang, H.-J. Moon, J. B. Lee, M. S. Bae, S. C. Lee, W. J. Lee, I.-C. Sun and I. K. Kwon, *Biomaterials*, 2012, **33**, 856.
- 14 A. Aykac, M. C. Martos-Maldonado, J. M. Casas-Solvas, I. Quesada-Soriano, F. García-Maroto, L. García-Fuentes and A. Vargas-Berenguel, *Langmuir*, 2014, **30**, 234.
- 15 N. Li, Y. Chen, Y.-M. Zhang, Y. Yang, Y. Su, J.-T. Chen and Y. Liu, *Sci. Rep.*, 2014, **4**, 4164.
- 16 T. Minko, P. V. Paranjpe, B. Qiu, A. Laloo, R. Won, S. Stein and P. J. Sinko, *Cancer Chemother. Pharmacol.*, 2002, **50**, 143.
- 17 A. M. C. Yvon, P. Wadsworth and M. A. Jordan, *Mol. Biol. Cell*, 1999, **10**, 947.
- 18 R. V. Chari, *Adv. Drug Delivery Rev.*, 1998, **31**, 89.
- 19 M. M. Alvarez, J. T. Khoury, T. G. Schaaff, M. N. Shafiqullin, I. Vezmar and R. L. Whetten, *J. Phys. Chem. B*, 1997, **101**, 3706.
- 20 (a) A. Elbakry, A. Zaky, R. Liebl, R. Rachel, A. Goepferich and M. Breunig, *Nano Lett.*, 2009, **9**, 2059; (b) G. Schneider and G. Decher, *Langmuir*, 2008, **24**, 1778.
- 21 C. M. Goodman, C. D. McCusker, T. Yilmaz and V. M. Rotello, *Bioconjugate Chem.*, 2004, **15**, 897.
- 22 J. M. Rosenholm, E. Peuhu, J. E. Eriksson, C. Sahlgren and M. Linden, *Nano Lett.*, 2009, **9**, 3308.
- 23 D. N. Heo, D. H. Yang, H. J. Moon, J. B. Lee, M. S. Bae, S. C. Lee, W. J. Lee, I. C. Sun and I. K. Kwon, *Biomaterials*, 2012, **33**, 856.